Kufa Journal of Engineering
Vol. 10, No. 3, July 2019, P.P. 1-18
Received 20 June 2018, accepted 25 September 2018

ANALYTICAL APPROACH TO PREDICT NONLINEAR PARAMETERS FOR DYNAMIC ANALYSIS OF STRUCTURES APPLIED TO BLAST LOADS

Ali N. Attiyah[1] and Hawraa M. Hussain[2]

[1] Assistant Professor of Civil Engineering, Faculty of Engineering, University of Kufa, Al-Najaf, Iraq. E-Mail: alin.diebil@uokufa.edu.iq

[2] M.Sc. Candidate, Civil Engineering, Faculty of Engineering, University of Kufa, Al-Najaf, Iraq. E-Mail: hawraa.mohammed.hussain@gmail.com

http://dx.doi.org/10.30572/2018/kje/100301

ABSTRACT

In this study, the Performance Based Design PBD method, which has been used only in seismic design by several codes, has been expanded to be applied to structures exposed to blast loads. The plastic hinge models used in PBD, which currently available for earthquake loads do not represent real behavior under the blast load. An analytical approach was proposed to represent the plastic behavior of flexural response under blast loads. The proposed model considers the following essential phenomena: concrete cover crushing, concrete core crushing, bar buckling in compression reinforcement, strain hardening in tensile reinforcement and softening in reinforcement bar. The proposed analytical approach has been validated with two experimental results of columns applied to blast loads and reasonable results has been seen

KEYWORDS: Performance Based Design PBD, plastic hinge, concrete cover crushing, concrete core crushing, bar buckling, blast loads, nonlinear dynamic analysis.

1. INTRODUCTION

Over the last few decades, the increasing of terrorist attacks on civilian buildings, led to growing research interests on the protection of civil facilities. In the case of severe loads, the design is based on deformation capacity, which is called Performance Based Design (PBD), instead of using strength capacity. Hence, in the present study, the PBD method will be used to investigate the blast resistance of structural components. For seismic design, there are several codes use the nonlinear dynamic analysis such as ASCE/SEI 41-13, PEER 2010, ACI 374.3R-16, FEMA 2012 and FEMA 2009 (Haselton, C.B. et al. 2016). To the authors knowledge, there are no code or research provide plastic hinge model for nonlinear dynamic analysis of structures applied to blast loads.

The seismic plastic hinge model was used in the nonlinear dynamic analysis in such cases, where the validity is questionable and need to be investigated. The researches done by Draganic and Sigmund, 2012, Kulkarni and Sambireddy, 2014, Vinothini and S. Elavenil, 2014, Priyanka and Rajeeva, 2015, and Shinde et al, 2016 are good examples of using seismic plastic hinge in dynamic analysis of structures applied to blast loads. The main objective of the present study are to apply the PBD philosophy to structural components subjected to external explosions.

2. ASCE 41-13 PLASTIC HINGE MODEL VALIDATION UNDER BLAST LOADS

ASCE 41-13, 2013 assumed that the nonlinear load-deformation relation is based on experimental evidence or taken from specified tables showing deformation limits. The typical ASCE 41-13 load-deformation relation is shown in Fig. 1, where deformations are expressed using terms, such as strain, curvature, rotation or elongation. Generally, the typical plastic hinge model is described by Modeling Parameters MPs and Acceptance Criteria (Ghannoum. W. M., 2014). The parameters (a) and (b), which can be found from ASCE 41-13 refer to post-yield deformation or plastic deformation. When the load-deformation relation is used to express the flexural response, it is given as moment-rotation relation for the plastic hinge at a section.

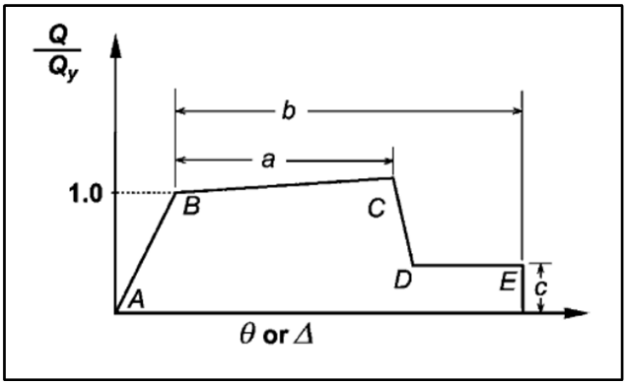

Fig. 1. ASCE 41-13 load-deformation relationship.

The ASCE 41-13 Plastic Hinge Model was applied to the column tested by Kadhom B., 2016. The column was tested up to flexural failure only without the influence of the axial force and its dimensions was 150×150×2230 mm. The column was constructed with seismically reinforcement details, which consist of Ø11.3 mm longitudinal reinforcement for each concrete column and ties reinforcement Ø6.3 mm spaced at 37.5mm center to center. Fig. 2 describes the details of reinforcing steel, and Table 1 shows its mechanical properties. Concrete cover from the outer edge of the ties was 10mm and the concrete compressive strength was 44MPa. The support conditions for these columns was simply supported. The amount of blast loads carried through the loading device (i.e. shock tube) on this column was 35kPa at duration of the positive phase 20ms, and its reflected impulse equals to 345.2 kPa.ms.

Table 1. Mechanical Properties of Reinforcement.

Properties of Reinforcement	10M (Ø11.3mm rebar)	Ø6.3mm smooth steel
Yield stress, fy (MPa)	572	521
Yield strain,εs	0.0025	0.0045
Ultimate stress, fu(MPa)	748	578
Ultimate strain,εu	0.0771	0.0405

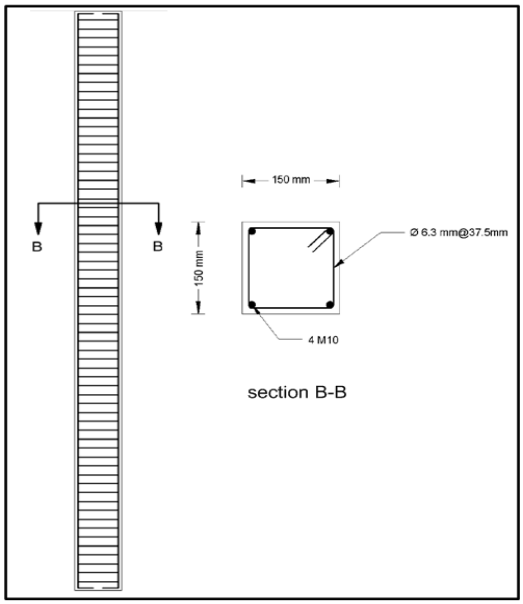

Fig. 2. Column dimensions and reinforcement detailing for Kadhom column.

In the current case study, the values of MPs according to ASCE 41-13 will be a=0.035, b=0.06 and c=0.2. ASCE 41-13 specifies flexural rigidity for columns with compression caused by design gravity loads ≤ 0.1Ag f`c corresponding to 0.3 Ec Ig. E=concrete modulus (taken as $57{,}000\sqrt{f'c}$ , psi), Ag=gross area of column cross-section, and f`c=concrete compressive strength. The slope of line BC, which represent the increase in strength due to hardening of reinforcement, shall be taken between zero and 10% of the initial slope according to ASCE 41-13. For more accurate calculations, the slope of line BC represent the difference between nominal strength, which is calculated from Eq. (1), and the probable strength which represents that associated with strain hardening of the steel reinforcement, i.e. 1.25 fy, which is calculated from Eq. (2). So, the slope of line BC will be equal to 1.25.

$$M_{ult} = A_s f_y (d - a/2) \quad (1)$$

$$M_{pr} = 1.25 A_s f_y (d - a/2) \quad (2)$$

$$a = \frac{A_s f_y}{0.85 b f'_c} \quad (3)$$

Where: $M_{ult.}$ = nominal moment, M_{pr}: probable moment, A_s = total area of tension reinforcement within the beam, fy = yield strength of reinforcement, which should be taken as F_{dy} for blast loads, d = distance from extreme compression fiber to centroid of tension reinforcement, a = depth of equivalent rectangular stress block, b = width of the column and f'_c = compressive strength of concrete, which should be taken as f'_{dc} for blast loads. Rotation at point (B) is

calculated from Eq. (4) (Elwood J. et. al., 2007). The MPs, ultimate strength and slope of line BC are defined as shown Fig. 3, and entered as the user defined plastic hinge in ETABS as shown in Fig. 4, and then the nonlinear dynamic analysis is performed.

$$\theta = \frac{M_{ult.}L}{3EI_{eff.}} \qquad 4$$

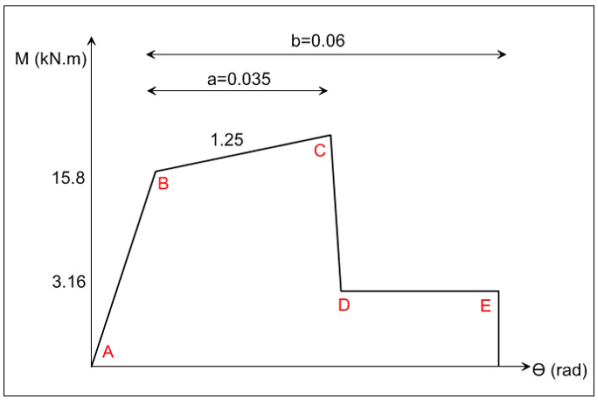

Fig. 3. ASCE 41-13 plastic hinge model of Kadhom's column.

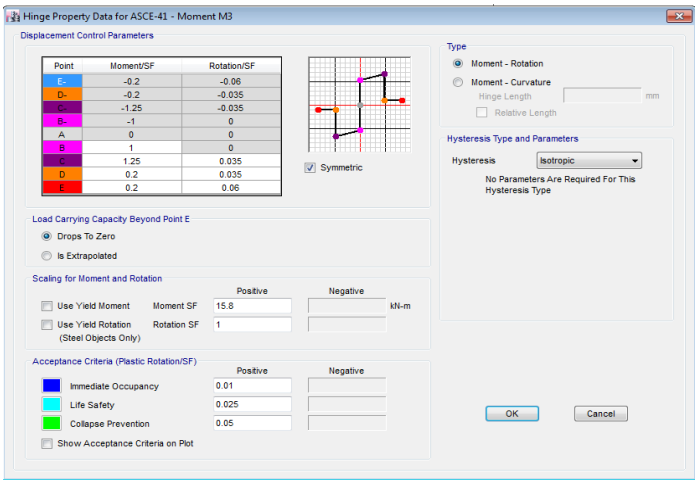

Fig. 4. Application of ASCE 41-13 Plastic Hinge Model for Kadhom's column by ETABS program.

Fig. 5 represents the comparison of displacement at the column mid-height between experimental and analytical results using ASCE 41-13 plastic hinge model. As shown in this figure, the column fails at low displacement value and do not represent the actual response of the experimental test. Fig. 6 shows the behavior of ASCE 41-13 plastic hinge, where it can be seen clearly that all the plastic hinge capacity will be exhausted within short time (i.e. 13 msec.), which is different from the experimental results (i.e. 48 msec.).

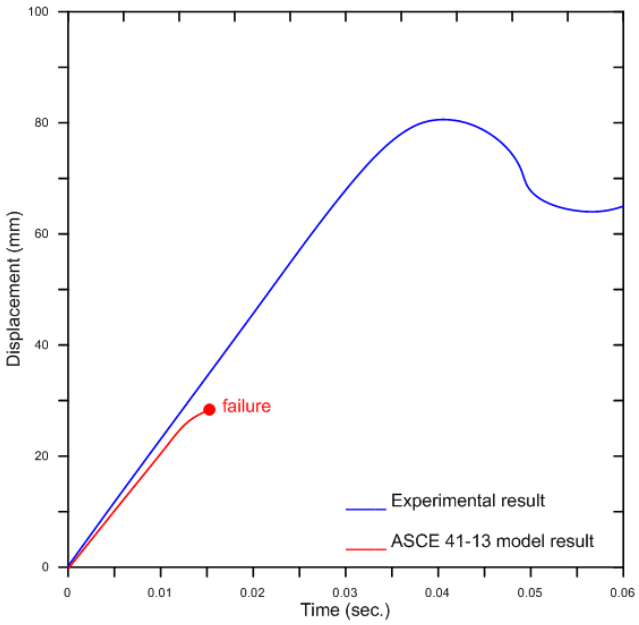

Fig. 5. Displacement time history for Kadhom's column by ASCE 41-13 plastic hinge model.

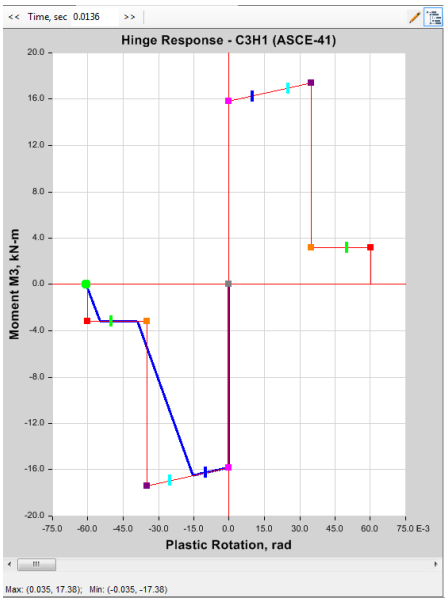

Fig. 6. ASCE 41-13 plastic hinge behavior for Kadhom's column.

3. PROPOSED PLASTIC HINGE MODEL

In order to produce an accurate and comprehensive plastic hinge model for the nonlinear dynamic analysis, understanding of important phenomena in the behavior of both materials concrete and reinforcement is required. The proposed model considers the following essential phenomena: concrete cover crushing, concrete core crushing, bar buckling in compression reinforcement, strain hardening in tensile reinforcement and softening in reinforcement bar. The models of concrete and reinforcement in tension and compression will be discussed in the coming sections.

3.1. Material Models and Material Properties

To establish the moment-rotation model of a concrete section, this requires calculating section properties based on material constitutive relations of concrete and steel, strain compatibility, and equilibrium (Shayanfar J., and H.A. Bengar, 2017). Thus, in the present section, the properties of materials which represent all the pre-and post-yield behavior are described.

i) Stress-Strain Model for Concrete

The modified Kent and Park model will be adopted in the present study. This model proposed by (Park et. al.1982) and was a modified method of the Kent and Park model published in 1971. Fig. 7 shows the modified Kent and Park model (Sharma A. et al., 2012).

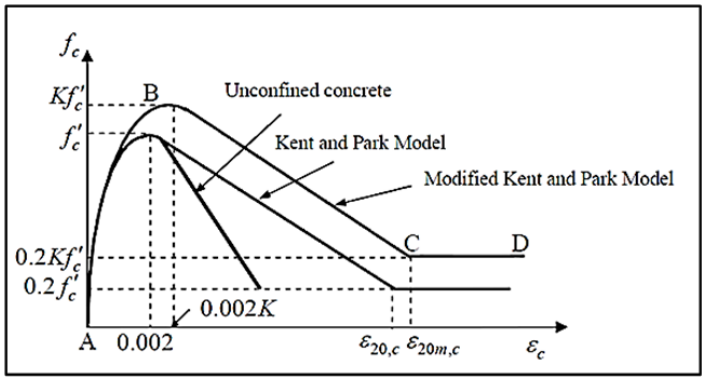

Fig. 7. Modified Kent and Park model for confined concrete (Sharma A. et al., 2012).

The model contained three parts of behavior, which can be defined in the following equations.

For region AB, $\varepsilon_c \leq 0.002K$

$$fc = k\, f`c \left[\frac{2\,\varepsilon_c}{0.002k} - \left(\frac{\varepsilon_c}{0.002k}\right)^2\right] \quad (5)$$

For region BC, $0.02k < \varepsilon_c < \varepsilon_{20m,c}$

$$fc = k\, f`c[1 - Z_m(\varepsilon_c - 0.002k)] \geq 0.2k\, f`c \quad (6)$$

Where:

$$z_m = \frac{0.5}{\frac{3+0.29\, f`c}{145\, f`c-1000}+0.75\rho_s \sqrt{\frac{b``}{s_h}}-0.002K} \quad (7)$$

For region CD,

$$fc = 0.2\, K\, f`c \quad (8)$$

Where:

$$k = 1 + \frac{\rho_s\, f_{yh}}{f`c} \quad (9)$$

$$\rho_s = \frac{2(b``+d``)A_s}{b``\, d``\, s_h} \quad (10)$$

f_{yh}: yield strength of steel hoops, f`c: concrete cylinder strength in MPa, A_s: cross sectional area of the stirrup reinforcement, ρ_s: the ratio of the volume of transverse reinforcement to volume of concrete core measured to outside of hoops, i.e, b``: width of confined core measured to outside of hoops, d``: depth of confined core measured to outside of hoops, S_h: spacing of hoops.

ii) Stress-Strain Model for Reinforcement

a) Reinforcement in Tension

The general form of strain-strain curve relationship for steel reinforcement in tension is represented by four regions: (1) linear elastic, (2) yield plateau, (3) strain hardening, and (4) post-ultimate stress region (Yu., W.,2006), as shown in Fig. 8.

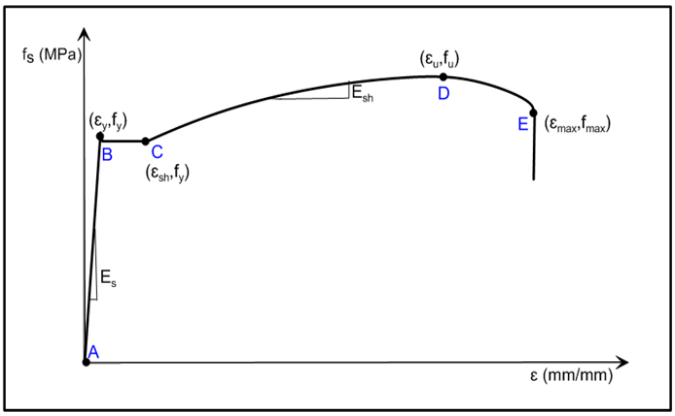

Fig. 8. General stress-strain curve for reinforcement.

Linear elastic region

The assumed stress-strain relation in this region is:

$$f_s = E_s \varepsilon_s \quad (11)$$

Yield plateau region

The idealized stress-strain relationship in this region is:

$$f_s = f_y \quad (12)$$

$$\varepsilon_y = \frac{f_y}{E_s} \quad (13)$$

Strain hardening region

The strain hardening zone ranges from the ideal coordinates that strain hardening begins, (ε_{sh}, f_y), to the ultimate coordinates, (ε_u, f_u) that correspond to the point that resists the maximum load and starting of the bar necking (Yu., W., 2006). The idealized stress-strain relationship in this region is represented by Eq. (14).

$$f_s = f_y + E_{sh}(\varepsilon_s - \varepsilon_{sh}) \quad (14)$$

Where: ε_s: steel strain, ε_y: yield strain, ε_u: ultimate steel strain, fs: steel stress, f_u: stress at the ultimate strain, E_s: modulus of elasticity of steel, and E_{sh}: strain hardening slope equal to $\frac{f_u - f_y}{\varepsilon_u - \varepsilon_{sh}}$.

b) Reinforcement in Compression

The stress-strain relationship of reinforcing steel in compression is the same as that in tension only, if the reinforcement was prevented from buckling (Dodd, L.L., and Restrepo-Posada, J.I, 1995). The modified Ohi and Akiyama model for bar buckling will be adopted in the present study (Kato et al., 1973). For monotonic loading, the buckling is assumed to begin at a critical buckling strain, ε_{lb}, indicated by point A as shown in Fig. 9. Post-buckling softening occurs by assuming, firstly, the stress decrease by $\tau_{lb}E_s$ until the strain reaches ε_{ps}. After that, the slope decreases by -0.005Es as shown Fig. 9. The term $\tau_{lb}E_s$ is calculated from Eq. (16). The value of ε_{ps} is equal to ε_{lb}+0.01. (Nakatsuka et al., 1999) relationship will be adopted to calculate the strain buckling ε_{lb} as shown in Eq. (15).

The relationship considers the effect of the following parameters: lateral reinforcement spacing to confined core diameter ratios; confining stress; yield strength of lateral reinforcement, f_{yh}; the shape of reinforcement (circular, rectangular); and the compressive strength of plain concrete. The bar buckling initially resisted by the lateral restraint provided by the concrete cover as well as the transverse reinforcement (Bai Z.Z. and Au, F., 2011).

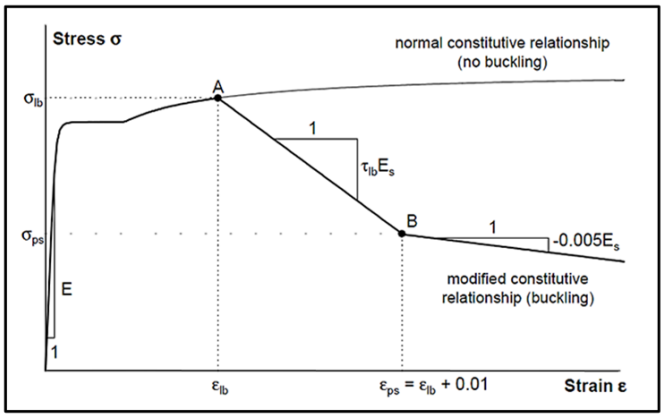

Fig. 9. Buckling model for monotonic behavior of compressive reinforcement.

$$\varepsilon_{bu=\varepsilon_{co}} + f_1 f_2 f_3 f_4 f_5 \quad (15)$$

Where, $f_1 = \begin{cases} 3.6 - 4.8\left(\frac{s}{d}\right) & 0.1 \le s/d \le 0.75 \\ 0 & s/d > 0.75 \end{cases}$

$$f_2 = (\rho_s f_{yh})^2$$

f_3 = 1.0 for bar in circular column; 0.9 for corner bar; 0.18 for intermediate bar

$$f_4 = \begin{cases} \frac{110}{fc} - 1 & for \quad 30MPa \le fc \le 110MPa \\ 0 & for \quad fc \ge 400MPa \end{cases}$$

$$f_5 = \left[\frac{600}{f_{yh}} + 0.5\right] \times 10^{-4} \qquad f_{yh} \ge 400MPa$$

where, d = smallest side length of the concrete cross section surrounded by lateral reinforcements, $f`_c$= cylinder concrete strength, ε_{c0} = maximum strain of plain concrete and ρ_s = reinforcement ratio of transverse reinforcement to concrete core.

$$\tau_{Ib} = 100\ \varepsilon_{sy}\ \left[\frac{1}{\sqrt{1+0.005\lambda^2}} - 1\right] \qquad 16$$

where, ε_{sy} = yield strain of longitudinal steel, $\lambda = \alpha s / ir$, α = 1.0 for corner bars; 0.5 for intermediate bars and ir = radius of gyration for bar.

3.2. Analytical Approach for Moment Rotation Behavior

The moment-rotation behavior represents the plastic hinge model for flexural action in Reinforced Concrete RC components under the effect of blast loads. In the previous studies, the moment-rotation was conducted until concrete core crushing (i.e. loss of the compression strength). The existence of the compression reinforcement in the section may increase the deflection until the bar buckling or rupture in tensile reinforcement occurs. Therefore, in the present study, the compression reinforcement role will be considered in the moment-rotation behavior in both pre- and post-concrete core crushing stages.

The proposed analytical approach is capable of predicting the concrete cover crushing, concrete core crushing, bar buckling in compression reinforcement, strain hardening in tensile reinforcement and softening in reinforcement bar (post-yield behavior), which produce the additional mechanism to dissipate the energy of components.

Pre-crushing of concrete core stage

In this stage, the plastic rotation until concrete core crushing is taken into account. It is known that the RC columns consist of unconfined cover concrete and confined concrete core. Under blast load effects, the concrete cover crushing occurs at the earlier stages, due to high rate in strain. Thus, the plastic behavior of the proposed model starts when the concrete cover reaches its ultimate strength (i.e. ultimate strain 0.003). So, the strength of concrete cover will be neglected and the symbols k and kd refer to the depth and neutral axis depth of confined

concrete core, respectively. Fig. 10 shows the strain diagram during the stage of pre-crushing of concrete core. The analytical approach is summarized in the following steps:

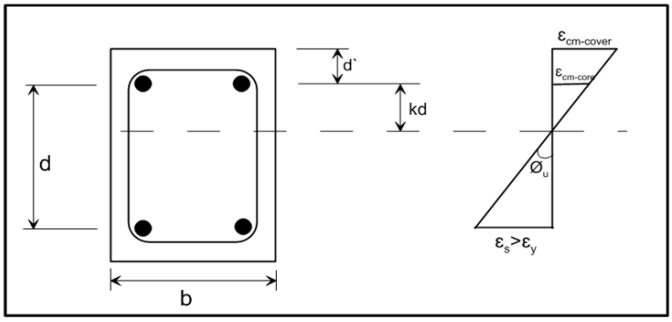

Fig. 10. Strain diagram in pre-stage of crushing core concrete.

1- Assume strain at the concrete cover $\varepsilon_{cm\text{-}cover}$ reaches the ultimate value 0.003.

2- Assume a value of neutral axis depth kd, starting from kd ≥0.5d.

3- Find the strain at extreme fiber of confined concrete $\varepsilon_{cm\text{-}core}$ by interpolation.

4- Determine the parameters of compressive stress block of concrete α and γ in region BC in the modified Kent and Park model which is shown in Fig. 7. Eqs. (17) and (18) are dependent on the values of $\varepsilon_{cm\text{-}core}$ and kd.

$$\alpha = \frac{1}{\varepsilon_{cm}}\left[\frac{0.004k}{3} + (\varepsilon_{cm} - 0.002k) - \frac{z_m}{2}(\varepsilon_{cm} - 0.002k)^2\right] \quad 17$$

$$\gamma = 1 - \frac{1}{\varepsilon_{cm}}\left[\frac{\left[\left\{\frac{\varepsilon_{cm}{}^2}{2} - \frac{(0.002k)^2}{12}\right\} - z_m\left\{\frac{\varepsilon_{cm}{}^3}{3} - 0.001k\varepsilon_{cm}{}^2 + \frac{(0.002k)^3}{6}\right\}\right]}{\left[\left\{\varepsilon_{cm} - \frac{0.002k}{3}\right\} - z_m\left\{\frac{\varepsilon_{cm}{}^2}{2} - 0.002k\varepsilon_{cm} + \frac{(0.002k)^2}{1}\right\}\right]}\right] \quad 18$$

Where k and Z_m were described in section 3.1.1.

5- Determine the total compressive force in concrete $C_{conc.}$ from the Eq. (19).

$$C_{conc} = \alpha f`_{dc}\, b\, kd \quad 19$$

Where $f`_{dc}$: dynamic strength of concrete, b: width of cross section, and kd: depth of neutral axis of concrete core.

6- Find strain of steel ε_{si} at different levels of section by interpolation depending on kd and $\varepsilon_{cm\text{-}core}$ values and calculate the corresponding stress in steel bars f_{si} using the stress-strain curve which discussed in section 3.1.2 part I.

7- Determine the tensile force in reinforcement T_s from Eq. (20).

$$Ts = f_{ds}\, A_s \quad 20$$

Where f_{ds}: dynamic strength of reinforcement, and A_s: area of reinforcement.

8- Check the equilibrium between compressive and tensile forces. If they are equal go to step 9, and if $C_{conc} > Ts$, decrease kd and return back to step 2, and if $C_{conc} < Ts$ go to step 13.

9- Calculate the moment, as follows:

$$M = Ts\ (D - \gamma kd) \quad (21)$$

Where

$$\mathrm{Ts} = \mathrm{f_{si}} \times A_{si} \quad (22)$$

fs; stress in bar, and As; area of bar

10- Calculate the curvature value, as follows:

$$\varphi_i = \frac{\varepsilon_{cm}}{kd} \quad (23)$$

11- Find rotation value, as follows:

$$\theta_i = \theta_y + (\varphi_i - \varphi_y) l_p \quad (24)$$

Where: $\theta_i = \frac{\varphi_y L_{eff}}{2}$ (25)

$\varphi_y = 2.14 \times \frac{\varepsilon_y}{D}$ Priestley et al. model (Shayanfar and Bengar, 2017) (26)

Where;

$L_{eff} = L + 0.022 f_s\, d_b$ Paulay and Priestley (Shayanfar and Bengar, 2017) (27)

L_p: plastic hinge length, and D: depth of the section.

12- Repeat steps 1-11 by increasing the value of $\varepsilon_{cm\text{-}core}$ with a specific increment such as 0.001, until the tensile force exceeds the compressive force.

At large compressive strain values, the tensile force exceeds the compressive force and the concrete core crushing occurs, which means losing the section ability to resist compression. This phenomenon occurs earlier under blast loads due to the high strain rate of the material. At this stage, the compressive strength is transferred to the reinforcing steel in the compression zone. Hence, in the blast-resistant structural components, concrete beams with tension reinforcement only are not permitted. Compression reinforcement, at least equal to one-half the required tension reinforcement, must be provided **(**Ho et al., 2005).

Post-crushing of concrete core stage

The following additional steps will describe the post-crushing stage of concrete as seen in Fig. 11.

13- Determine the buckling strain of compression reinforcement from Eq. (15), which was referred to in section 3.1.2, part II.

14- If the strain of steel, which will be referred by ε_{s-h} in this stage, is smaller to the buckling strain ε_{bu}, then, the stress of steel increased duo to the hardening corresponding to the stress-strain curve for reinforcement. Otherwise the stress of steel decrease by $\tau_{lb}E_s$ until the strain of steel reaches ε_{ps}. After that, the slope decreases by 0.005Es. The values of ε_{ps}, $\tau_{lb}E_s$, and ε_{bu} were discussed in section 3.1.2, part II.

15- Find moment from Eq. (28): (UFC3-340-02, 2008)

$$M = As \times f_{ds} \times d \quad (28)$$

Where M is the moment at the post-crushing of concrete core stage, As is the total area of tension reinforcement within the beam, f_{ds} is the dynamic design stress of reinforcement, and d is the distance between the compression and tension reinforcement.

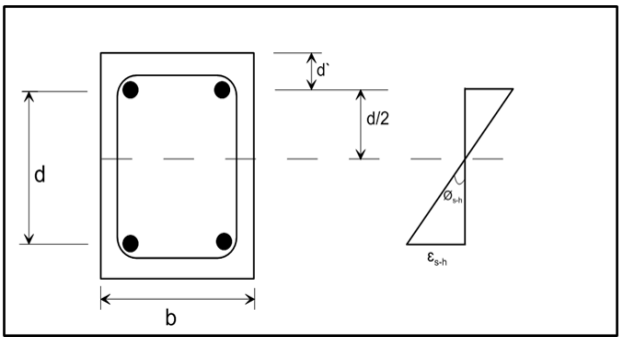

Fig. 11. Strain diagram in post-stage of crushing core concrete.

16- Calculate the curvature $Ø_{s-h}$ from Equation (29)

$$\varphi_{s-h} = \frac{\varepsilon_{s-h}}{(d-d`)/2} \quad (29)$$

Where ε_{s-h}: hardening strain reinforcement.

17- Calculate the rotation in this stage $\Theta_{hard.}$. from Eq. (30).

$$\theta_{hard.} = (\varphi_{s-h} - \varphi_u) l_h \quad (30)$$

Where $Ø_{s-h}$: curvature of reinforcement in post-crushing of concrete core stage, $Ø_u$: ultimate curvature at which concrete core crushing occur, and L_h: hardening hinge length. A part of the plastic hinge zone is assumed as the region over which the longitudinal reinforcement hardening, which is called L_h as shown in Fig. 12. Hardening hinge length will be assumed to be equal to H/2, which its validity will be checked later.

Where H is the depth of section.

18- Calculate total rotation Θ_{s-h} from Eq. (31)

$$\theta_{s-h} = \theta_{hard.} + \theta_{ult.} \quad (31)$$

Where $\Theta_{s\text{-}h}$: ultimate rotation in post-crushing of concrete core stage.

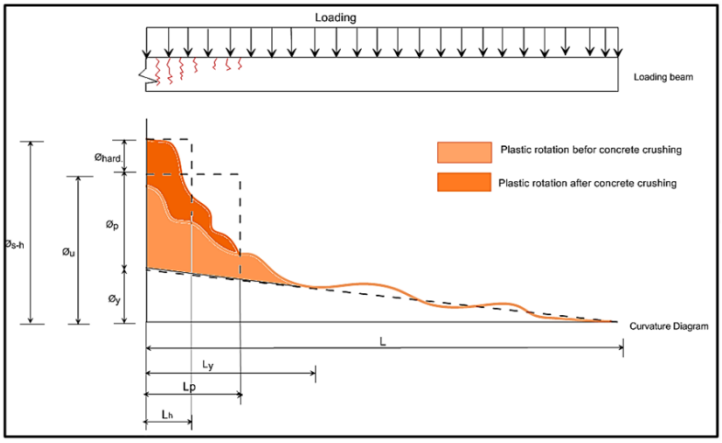

Fig. 12. Curvature diagram in pre-and post-concrete crushing stages.

19- Repeat steps 14-18 by increasing the value of $\varepsilon_{s\text{-}h}$ with a specific increment such as 0.001 until reaches the dynamic ultimate stress of reinforcement f_{du}.

3.3. Validation of the Proposed Analytical Approach

The proposed analytical approach was validation with the experimental program of Kadhom B., 2016. Fig. 13 displays the complete moment-rotation relationship conducted using the analytical approach mentioned in section 2.2. The figure covers all strains, starting with the strain of concrete cover crushing until the ultimate strain of steel, using element geometry and reinforcement details of Kadhom's column.

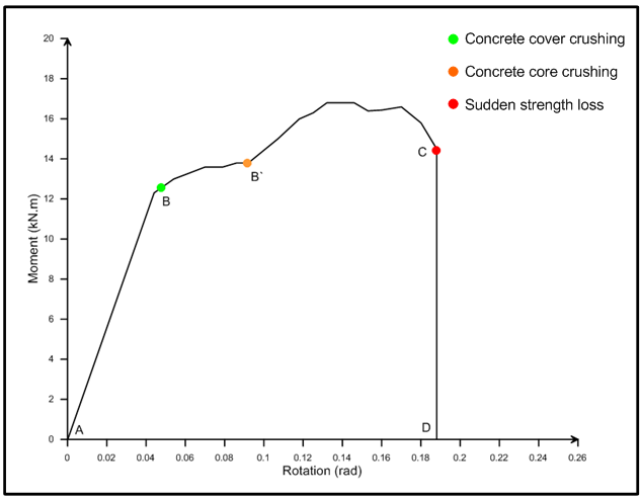

Fig. 13. Moment rotation curve for Kadhom's column.

The moment-rotation behavior is described by a series of points A, B, B`, C and D. Point (A) refers to the origin or unloading state, and point (B) refers to the crushing of concrete cover, which occurs at the ultimate strain of extreme fiber of concrete. Strain in this point equals to 0.003 according to ACI 318-14. The flexural strength and plastic rotation using the mentioned

procedure are found. Point (B`) refers to the concrete core crushing, which occurs when the tensile force exceeds the compressive force and concrete loses its strength. The compression strength in this stage transferred to compression reinforcement. At the same time, the strain hardening begins and the strength will be increased with the increase in deflection. Point (C) refers to the end of the reinforcement hardening due to the absence of buckling in compression reinforcement in this element. As mentioned earlier the compression reinforcement behaves similarly to tension reinforcement in the absence of bar buckling. At the end of the hardening, sudden strength loss occurs and the curve reaches point (D).

The moment-rotation behavior will be approximated to find a plastic hinge model that can capture the important plastic response phenomena, as shown in Fig. 14. The modeling parameters a and b of this model are similar and equal to 0.15 rad. The slope of line BC can be determined by dividing the ultimate strength at point (C) by the strength at point (B), which in this model equals to 1.3. The proposed model was used in ETABS as user-defined plastic hinge as shown in Fig. 15, and then nonlinear dynamic analysis is performed.

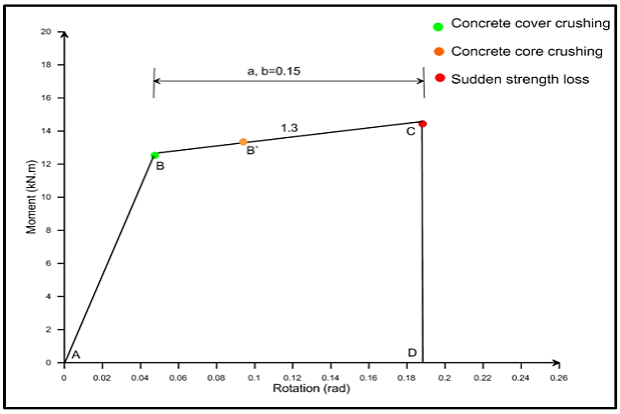

Fig. 14. Proposed plastic hinge model for Kadhom's column.

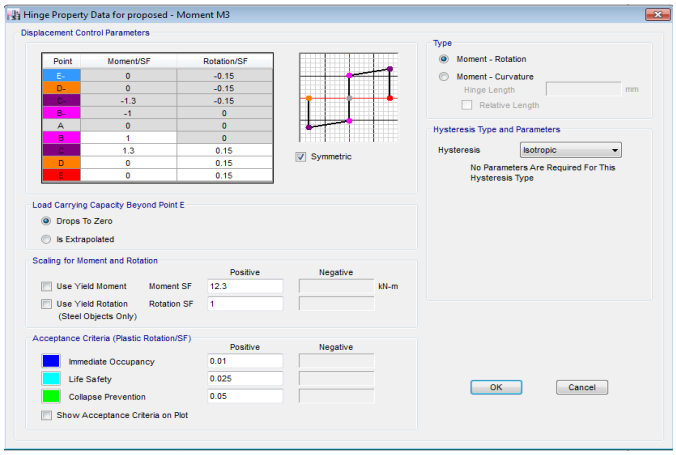

Fig. 15. Application of the proposed model by ETABS program.

Fig. 16 presents the comparison of displacement-time history of experimental and proposed model for Kadhom's columns. The results indicate the ability of the proposed model to represent the real response under explosion loads. Fig. 17 demonstrates the behavior of the proposed plastic hinge for Kadhom's columns. The response behavior in the plastic hinge model exceeds the concrete cover crushing as well as the concrete core crushing but don't reaches the failure of section.

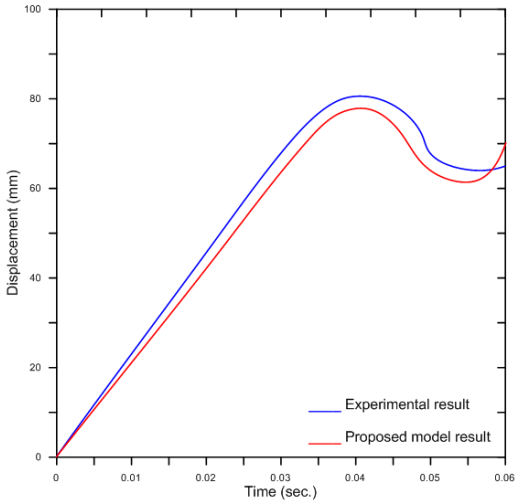

Fig. 16. Comparison between proposed plastic hinge model and experimental results.

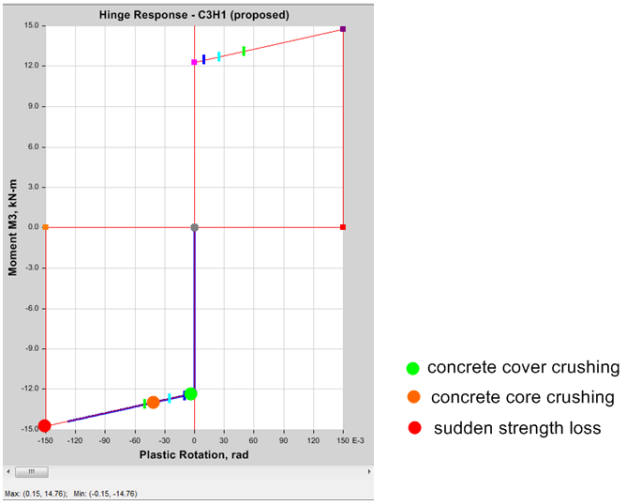

Fig. 17. Proposed plastic hinge behavior for Kadhom's column.

4. CONCLUSION

The following points are concluded from the present research:

1. The seismic plastic hinge characteristics of ASCE 41-13 are not valid in nonlinear dynamic analysis of structural components applied to blast loads.
2. An analytical approach was proposed that simulates real behavior under explosive loads. The proposed model considers the following essential phenomena: concrete cover crushing,

concrete core crushing, bar buckling in compression reinforcement, strain hardening in tensile reinforcement and softening in reinforcement bar.

3. The proposed model gives the opportunity for more understanding of the real failure modes of concrete members under the effect of blast loads, which may lead for more reliable strengthening and repair in such cases.

5. REFERENCE

American Society of Civil Engineers. ASCE/SEI 41–13 (2014), "Seismic Evaluation and Retrofit of Existing Buildings", Reston, United States.

Bai Z.Z. and Au, F. (2011), "Effects of Strain Hardening of Reinforcement on Flexural Strength and Ductility of Reinforced Concrete Columns", The Structural Design of Tall and Special Buildings, Volume 20, Issue 7, pp. 784-800.

Dodd, L.L., and Restrepo-Posada, J.I. (1995), "Model for Predicting Cyclic Behaviour of Reinforcing Steel," Journal of Structural Engineering, ASCE, Vol. 121 No. 3, pp. 433-445.

Draganić, H. and Sigmund, V. (2012), "Blast Loading on Structures", Tehnički Vjesnik Volume 19, Issue 3, pp. 643-652.

Elwood J. et al. (2007), "Update to ASCE/SEI 41 Concrete Provisions", Earthquake Spectra, Volume 23, No. 3, pp. 493–523.

Ghannoum. W. M. (2014), "Seismic Assessment of Existing Reinforced Concrete Buildings - New Developments", ACI Spring 2014 Convention.

Haselton, C.B. et al. (2016), "Guidelines on Nonlinear Dynamic Analysis for Performance-Based Seismic Design of Steel and Concrete Moment Frames", Proceedings of SEAOC 2016 Convention.

Ho J. et al. (2005), "Effects of strain hardening of steel reinforcement on flexural strength and ductility of concrete beams". Structural Engineering and Mechanics, Volume 19, Issue 2, pp. 185-198.

Kato, B. et al, (1973), "Predictable Properties of Material Under Incremental Cyclic Loading", IABSE, Report of the Working Commissions, Band 13, Symposium on Resistance and Ultimate Deformability of Structures Acted on by Well Defined Repeated Loads, Lisbon, pp. 119-124.

Kulkarni A. V. and Sambireddy, G. (2014), "Analysis of Blast Loading Effect on High Rise Buildings", Civil and Environmental Research, Volume 6, No. 10, pp. 2225-0514.

Nakatsuka, T. et al., (1999), “Equations to Estimate Strains at Buckling of Longitudinal Reinforcement Under Uniaxial and Monotonical Compression”, Journal of Structural and Construction Engineering, AIJ, No. 516, 145-149.

Priyanka A. and Rajeeva S. V. (2015), “Lateral Stability of a Multi-story Building under Blast Load”, IJRET: International Journal of Research in Engineering and Technology, Volume 04, Special Issue 14.

Shinde N.N. and Prasad R. (2016), “Comparative Study of Earthquake and Blast Load on Commercial Building”, International Journal of Scientific Research in Science and Technology IJSRST, Volume 2, Issue 3, pp. 34-38.

Kadhom, B. (2016), "Blast Performance of Reinforced Concrete Columns Protected by FRP Laminates ", M. Sc. Thesis Department of Civil Engineering Faculty of Engineering University of Ottawa, Canada.

Shayanfar J., and H.A. Bengar (2017), “Nonlinear analysis of RC frames considering shear behavior of members under varying axial load”, Bulletin of Earthquake Engineering, Volume 15, Issue 5, pp 2055–2078.

Sharma A. et al., 2012, “Nonlinear seismic analysis of reinforced concrete framed structures considering joint distortion”, Scientific Information Resource Division, Bhabha Atomic Research Centre, Mumbai.

Unified Facilities Criteria (UFC) UFC 3-340-02, (2008), “Structures to Resist the Effects of Accidental Explosions”, Unified Facilities Criteria, Department of Defense DoD, USA.

Vinothini P. and Elavenil S. (2016), “Analytical Investigation of High Rise Building under Blast Loading”, Indian Journal of Science and Technology, Volume 9, Issue 18.

Yu., W. (2006), “Inelastic modeling of reinforcing bars and blind analysis of the benchmark tests on beam column joints under cyclic loading”, M.Sc. dissertation, ROSE School, Pavia, Italy.